

Triplet exciton dynamics in rubrene single crystals

Aleksandr Ryasnyanskiy and Ivan Biaggio

Department of Physics, Lehigh University, Bethlehem, Pennsylvania 18015, USA

(Received 10 May 2011; revised manuscript received 25 October 2011; published 14 November 2011)

The decay of the photoluminescence excited in rubrene single crystals by picosecond pulses is measured over 7 orders of magnitude and more than 4 time decades. We identify the typical decay dynamics due to triplet-triplet interaction. We show that singlet exciton fission and triplet fusion quantum yields in rubrene are both very large, and we directly determine a triplet exciton lifetime of $100 \pm 20 \mu\text{s}$, which explains the delayed buildup of a large photocurrent that has been reported earlier for low excitation densities.

DOI: [10.1103/PhysRevB.84.193203](https://doi.org/10.1103/PhysRevB.84.193203)

PACS number(s): 72.80.Le, 71.35.-y, 72.40.+w, 88.40.jr

Photoluminescence dynamics in organic molecular crystals can provide information on the nature of excitons and their evolution from the initial photoexcitation to interaction with defects and ultimately to dissociation or recombination. Excitons in molecular crystals are of fundamental interest and their possible dissociation into free carriers is of relevant practical importance for optoelectronic applications such as photovoltaics. In particular, the rubrene single crystal has an extraordinarily large carrier mobility observed in field effect transistors,¹⁻³ and it is characterized by a large photoconductivity appearing with a rise time of $100 \mu\text{s}$ after impulsive excitation,^{4,5} which implies that a significant fraction of the photoinduced excitons in rubrene ultimately leads to mobile charge carriers.⁵ Even though the exciton dissociation mechanism has been associated both with oxygen-related defects^{5,6} and the crystal's surface,⁷ the path that leads from photon absorption to delayed carrier release in rubrene has not been fully described yet.

The initially photoexcited species in molecular crystals are singlet excitons with a lifetime of the order of nanoseconds or less. Under pulsed illumination, their radiative recombination leads to a photoluminescence (PL) signal that decays during the singlet lifetime. But in addition to this, creation of triplet excitons^{8,9} can lead to a long-lived PL signal because of their long lifetime and their capability of fusing together to regenerate a singlet state that can radiatively recombine.¹⁰ Most of the work in this field has concentrated on aromatic single crystals such as anthracene,^{8,9} tetracene,¹⁰ and naphthalene.¹¹ For rubrene, we are only aware of studies of delayed PL dynamics that were performed on molecules in solution.¹²

In this work we investigate delayed PL dynamics in vapor transport grown, orthorhombic rubrene single crystals, varying from pristine as-grown samples to samples that have been exposed to air and light for a long time. The rubrene PL spectrum has prominent emission bands near 560 nm and 608 nm.^{6,13} The amplitudes of smaller bands around 645 nm and beyond are more sample dependent and have been partially assigned to oxidation.^{6,13,14} We first studied the PL dynamics using 1 ps long pulses obtained from a Light Conversion TOPAS (traveling-wave optical parametric amplifier system) pumped at 1 kHz by a Clark-MXR Ti:sapphire amplifier. We used pulses at a wavelength of 420 nm (absorption length of $\sim 3 \mu\text{m}$) and with an energy of the order of $1 \mu\text{J}$ focused to a spot-size of $40 \mu\text{m}$ on the *ab* surface of the crystals, paying attention to avoiding any surface imperfections. We detected

the PL in a confocal geometry with a photomultiplier tube (PMT) connected to a 4 GHz LeCroy digital oscilloscope. Following excitation, we observed a fast PL component (inset in Fig. 1) that decays in less than 10 ns (limited by the time resolution of our equipment), followed by a slower component. The time dynamics of the slower component is shown in Fig. 1 for three wavelengths close to the most important bands in the rubrene PL spectrum. The wavelengths were selected by bandpass filters with a spectral width of 10 nm. The time-dependent data were obtained by combining several measurements taken at different time delays with a Hamamatsu gated PMT while keeping similar PMT output voltages to avoid saturation effects. The three decays are very similar to each other. In particular, the band at 645 nm, which has been argued to grow with oxidation,^{6,13,14} decays in the same way as the other bands over multiple time decades. This behavior remained the same among various samples where the prominence of the 645 nm band was different.

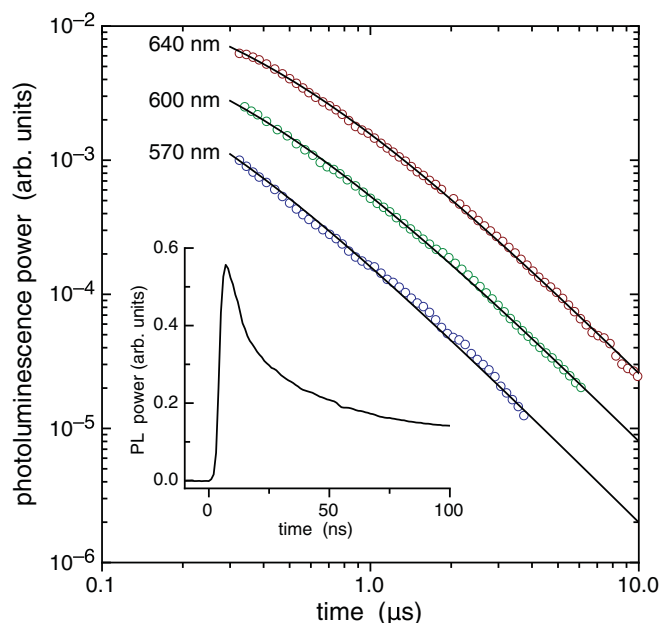


FIG. 1. (Color online) Rubrene PL dynamics for different wavelengths in the emission spectrum. Data sets for different wavelengths are shifted vertically for clarity. Solid lines are fits to the square of Eq. (2) in the limit $\tau_T \rightarrow \infty$. The inset shows the PL dynamics right after pulsed illumination.

The PL dynamics in Fig. 1 is clearly nonexponential and trends to a power law t^{-2} . In fact, this type of PL decay can be recognized as an example of the well-known situation where the singlet excitons initially created by the laser pulse transform into triplet excitons, which then mainly decay by triplet-triplet collisions that can recreate singlets.^{8,15,16} Thus, while the initial PL decay in Fig. 1 is due to radiative emission from singlet excitons created by the pump pulse, happening within a singlet lifetime τ_S of less than 10 ns, the remaining decay is due to emission from singlets that have been formed again later through triplet-triplet fusion.¹⁶ The fact that the PL intensity tracks the triplet density has also allowed us to directly observe triplet diffusion in rubrene.¹⁷ In the following, we discuss quantitatively the delayed PL dynamics expected because of these effects.

Before proceeding, we stress that the focus of this investigation is the time-evolution of the delayed PL. This PL is an observable that is proportional to the number of singlet excitons created per unit time, independently of the precise value and nature of the singlet-exciton lifetime, and of the mechanism with which an individual singlet exciton ultimately leads to some radiated PL. In this context, any complexity in the decay mechanisms of the singlet excitons^{18,19} does not affect our results. Further research will be needed to understand in general the relative role of the possible relaxation processes of photoexcited states, such as radiative recombination, dissociation into free carriers, or fission into triplets.

The time evolution of the triplet density T can be described by

$$\frac{dT}{dt} = (2f_S + \kappa)\frac{S}{\tau_S} - \frac{T}{\tau_T} - \gamma T^2, \quad (1)$$

where S is the singlet density, τ_S is the singlet lifetime, f_S is the probability for a singlet to undergo fission into two triplets, κ represents other possibilities for singlet-triplet conversion, τ_T is the triplet lifetime, and γ is a bimolecular interaction rate. For short singlet lifetimes ($\tau_S \ll T^{-1}\gamma^{-1}$ and $\tau_S \ll \tau_T$) and for $t \gg \tau_S$, the singlet density remains small compared to the triplet density $T(t)$. Equation (1) without the first term on the right-hand side has the analytical solution

$$T(t) = T_0[(1+r)e^{t/\tau_T} - r]^{-1}, \quad (2)$$

where $r = T_0\gamma\tau_T$. Note that the time dependence of $T(t)$ goes from a power law of the form $T(t) \sim (1 + T_0\gamma t)^{-1}$ at short times to an exponential $T(t) \sim \exp(-t/\tau_T)$ when t/τ_T becomes of the order of r or 1, whichever is smaller.

The delayed PL is due to the emission from a singlet population that evolves as $dS/dt = -S/\tau_S + f_T\gamma T^2/2$, where the last term describes triplet-triplet fusion, with f_T the probability that triplet-triplet interaction results in the creation of a singlet.¹⁶ It is important to note that triplet fusion can lead to singlet excitons and PL emission even in the case where the triplet density is so low that its decay is exponential, determined by the linear term T/τ_T in Eq. (1). Since the rate at which singlets are created is always proportional to γT^2 , the delayed PL power is proportional to T^2 , the square of the triplet density.¹⁶ At higher triplet density and for $t \ll \tau_T$ the PL follows the power law $(1 + T_0\gamma t)^{-2}$, which in a double-logarithmic plot becomes a straight line with a slope of -2 for $t > (T_0\gamma)^{-1}$ (see Fig. 1). The data show that the triplet

lifetime must be longer than 10 μs , and can be easily fitted by the power law $(1 + T_0\gamma t)^{-2}$ with $T_0\gamma = (3-6) \times 10^6 \text{ s}^{-1}$ (solid curves in Fig. 1). The data were collected in different runs, with possible fluctuations in T_0 and other noise sources causing slight differences in the initial slope of the data between the three wavelengths, but all three data sets clearly tend to the expected straight line with a slope of -2 at longer times. Next, we extend the experiments to determine the triplet lifetime.

In order to obtain a large enough signal-to-noise ratio to follow the PL decay beyond 10 μs it is necessary to decrease the initial density of triplet excitons while keeping the total number of absorbed photons large. We achieved this by illuminating a large rubrene crystal with unfocused (2 mm diameter) 20 ps, 40 μJ laser pulses at 10 Hz obtained from an Ekspla optical parametric generator at a wavelength of 530 nm, giving a longer absorption length of $\sim 10 \mu\text{m}$. In addition, we detected the whole PL spectrum with a long-pass filter. The results are shown in Fig. 2. The PL decay clearly becomes exponential at longer times, with the triplet lifetime coinciding with the deviation of the data from the straight line with a slope of -2 that occurs at times longer than 50 μs (indicated by the arrow). The inset in Fig. 2 shows a conventional semilogarithmic plot of the same data highlighting the exponential decay obtained at longer times, which has an exponential decay constant of $50 \pm 10 \mu\text{s}$. Because the PL is proportional to $T(t)^2$, this gives a triplet lifetime $\tau_T = 100 \pm 20 \mu\text{s}$, which is similar to that observed earlier in rubrene solutions.^{12,20,21}

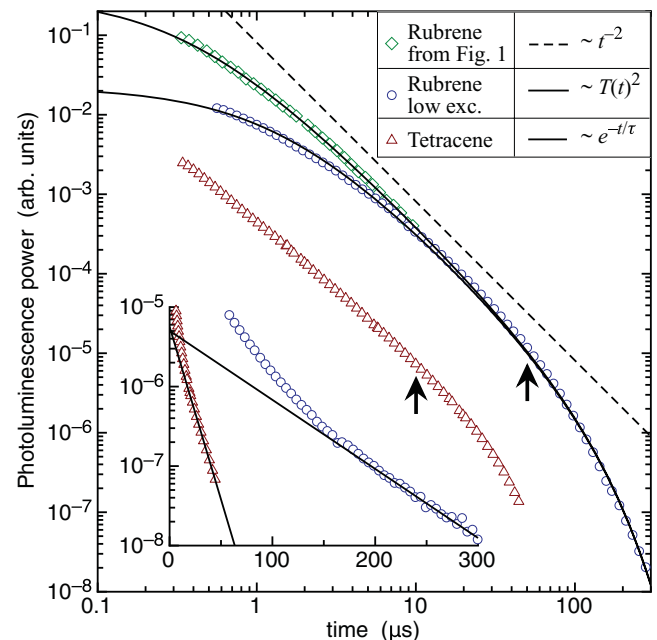


FIG. 2. (Color online) Delayed PL dynamics in rubrene and tetracene. The solid curves are fits to the square of Eq. (2). The dashed line has a slope of -2 , for reference. The inset is a semilogarithmic plot of the same data. The dash-dotted lines are exponential decays $\exp(-t/\tau)$, with $\tau = \tau_T/2 = 50 \mu\text{s}$ for rubrene and $\tau = 10 \mu\text{s}$ for tetracene.

The complete PL decay of Fig. 2, including both power-law and exponential parts, can be fitted using $T(t)^2$ as given by the analytical solution in Eq. (2). The best fit is obtained for $T_0\gamma = 7.0 \times 10^5 \text{ s}^{-1}$ and $\tau_T = 100 \text{ } \mu\text{s}$ (corresponding to $r = 70$). We note that this fit uses only two fittable parameters, and that the agreement with the data is very good over 7 orders of magnitude and more than 4 time decades. In addition to the clearly identifiable power law that then converts into an exponential decay, this is a very strong proof of the validity of the model leading to Eq. (2). The value of $T_0\gamma$ used here is 5 times smaller than for the fits in Fig. 1, corresponding to the modified exposure conditions and lower triplet density. Figure 2 also includes the 640 nm data from Fig. 1, fitted in the same way by just appropriately increasing T_0 , further confirming the robustness of the model. Using an upper limit for T_0 of 10^{18} cm^{-3} —estimated from the number density of absorbed photons—we find a lower limit for the bimolecular recombination constant of $\gamma_{\text{MIN}} = 7 \times 10^{-13} \text{ cm}^3 \text{ s}^{-1}$, consistent with the earliest measurements in tetracene and anthracene.^{8,15,16}

We also included in Fig. 2 the PL decay we measured in the same way in tetracene. The data are qualitatively very similar to rubrene, with a similar power-law decay, but with a slope slightly smaller than 2, for which reason we did not fit it through Eq. (2). The smaller slope could be due to inhomogeneities near the crystal surface causing the PL decay to be a superposition of several behaviors. In any case, even though we could not follow the decay further than $50 \text{ } \mu\text{s}$ because of low signal-to-noise ratios, the data clearly indicate a triplet lifetime of $20 \pm 5 \text{ } \mu\text{s}$, with a deviation from the power-law decay occurring around $10 \text{ } \mu\text{s}$. This is consistent with a report of a delayed fluorescence lifetime of $5\text{--}10 \text{ } \mu\text{s}$ in tetracene.²²

The data presented above allow for several important insights. First, we already mentioned that the time-evolution for different wavelengths of the delayed PL is essentially the same, including emission bands that have been associated with defects (Fig. 1). It follows that the PL associated with defects must also originate from the triplet population, probably by a mechanism where the singlet excitons obtained through triplet fusion interact with defect states.

Second, a simple analysis of the PL time dynamics reported above allows us to evaluate the efficiency of the singlet-to-triplet and triplet-to-singlet conversion mechanisms responsible for the delayed PL. We find that under relatively high excitation densities like those used for the data in Fig. 1, the time integral of all the observed delayed PL power, from 10 ns after excitation to the final exponential decay, is at least ~ 25 times larger than the time integral of the initial PL emitted by the photoexcited singlets. Under these circumstances the vast majority of the initially created triplets are destroyed via the bimolecular process that can create singlet excitons again. The fact that more than 95% of all PL photons can be emitted via triplet-triplet interaction means that the combined process of singlet-to-triplet and triplet-to-singlet conversion must be very efficient in rubrene. The only physical process that can account for such an efficient singlet-to-triplet transition is the spin-allowed exciton *fission* process.^{16,23–25} Assuming a probability f that a singlet recombines radiatively and a high-density situation where every triplet is bound to interact with another triplet, we can quantify the delayed PL signal

from the probability f_S that a singlet undergoes fission into two triplets and the probability f_T that triplet-triplet annihilation results in a singlet. For an initial number of singlets N , the total number of emitted PL photons is proportional to $Nf[1 + f_T f_S + (f_T f_S)^2 + (f_T f_S)^3 + \dots]$ and the ratio between total integrated PL and PL emitted by the initially photoexcited singlets is

$$R = 1 + f_T f_S + (f_T f_S)^2 + \dots = [1 - f_T f_S]^{-1}. \quad (3)$$

This can only become as large as the $R \sim 25$ we have measured if both f_T and f_S are close to unity. Such efficient fusion and fission quantum yields, combined with the short singlet lifetime, mean that triplet collision will often result in a singlet that again undergoes fission to form triplets, a process that at high excitation densities can be repeated several times until finally the singlet exciton recombines. The conclusion that *both* exciton fission and fusion are very efficient in rubrene is logically required to explain the PL data with the exciton dynamics model presented here, and is valid for our relatively low singlet photoexcitation densities. It implies that the energy of triplet excitons in rubrene must be close to half the singlet energy; if this was not the case one of the two processes would need significant phonon assistance, leading to a lower probability for either fission or fusion. This result agrees with Ref. 12, which concluded from solution studies that the triplet energy of rubrene should be virtually half that of the singlet, and with Ref. 26, which reported a triplet energy of $\sim 1.2 \text{ eV}$ and a singlet energy of $\sim 2.33 \text{ eV}$. We also mention that singlet fission occurs efficiently in pentacene but needs thermal assistance in tetracene,²⁵ and variations in the intermolecular coupling can have a sizable effect on the fission efficiency.²⁷ Finally, both triplet fusion and efficient singlet fission have also been observed in rubrene in Ref. 24. At the end it is not surprising that in rubrene we find a peculiar balance between singlet and triplet exciton energies that leads to the rather interesting case of a simultaneously high probability for singlet fission, and for triplet-triplet annihilation leading to fusion into one singlet.

Third, direct electrical measurements in rubrene have shown that, at absorbed photon densities that are about 2–3 orders of magnitude smaller than those that we used to observe the PL dynamics, impulsive excitation is followed by a delayed release of free charge carriers.^{4,5,28} The exponential rise time of this carrier density matches the triplet lifetime we have determined here. One must therefore investigate the possibility that triplet excitons can dissociate into charge carriers at the low densities that make triplet-triplet interaction negligible. Despite their large binding energy, triplet dissociation could happen through secondary processes²⁹ involving defects.³⁰ An example could be Auger-like dissociation,^{31,32} where the electron from the exciton is captured by oxygen-related band-gap states⁶ and the energy gained in this way is used to excite the hole into the valence band. Because of the large carrier lifetime of several milliseconds,⁴ such a triplet dissociation process would lead to an initial rise in photoconductivity $\sigma(t)$ that is proportional to the time integral of the $T(t)$ given in Eq. (2):

$$\sigma(t) \propto \int_0^t T(u) du = \frac{1}{\gamma} \ln[(1+r)e^{t/\tau_T} - r] - \frac{t}{\gamma\tau_T}, \quad (4)$$

with a final value $\sigma(\infty) \sim \gamma^{-1} \ln(1+r)$ that corresponds to a linear dependence of the photoconductivity amplitude on the initial triplet density for low densities, and to a sublinear logarithmic growth at higher densities where $r > 1$. The time needed for the buildup to reach a fraction q of its final value is

$$t_0 = -\tau_T \ln\{1 + r^{-1}[1 - (1+r)^q]\}, \quad (5)$$

which at low excitation densities ($r \ll 1$) is a constant $t_0 = -\tau_T \ln(1-q)$, giving an exponential buildup with time constant τ_T , and at higher excitation densities ($r \gg 1$) can be expanded to give $t_0 \approx \tau_T(r^{q-1} + r^{2(q-1)}/2 + \dots)$, and hence a buildup rate $1/t_0$ proportional to r^{1-q} . At higher excitation densities more triplets are lost to bimolecular interaction before they can dissociate into charge carriers, leading to a saturation of the photocurrent amplitude that is accompanied by a faster buildup time. For $r \gg 1$, Eq. (5) gives a buildup rate for 50% of the final amplitude that grows as the square root

of the excitation density ($r^{1-q} \sim \sqrt{T_0}$ for $q = 0.5$). These predictions are exactly what was observed in Ref. 5, giving strong support to the idea that the delayed photocurrent in rubrene is caused by triplet exciton dissociation.

In conclusion, we followed the delayed PL decay in rubrene until 300 μ s after pulsed photoexcitation and determined that it results from the evolution of a triplet population created from the photoinduced singlet excitons by singlet-exciton fission. We found that in rubrene both the fission and the fusion quantum yields must be large and we determined a triplet lifetime of $100 \pm 20 \mu$ s. Finally, we showed that the efficient fission into triplets is responsible for the strong delayed photocurrent observed earlier,^{4,5} which we can now assign to triplet dissociation, with a saturation behavior at higher excitation densities that is caused by triplet-triplet interaction.

We thank V. Podzorov for the rubrene and tetracene samples and P. Irkhin for helpful discussions.

-
- ¹V. Podzorov, V. Pudalov, and M. Gershenson, *Appl. Phys. Lett.* **82**, 1739 (2003).
²R. de Boer, M. Gershenson, A. Morpurgo, and V. Podzorov, *Phys. Status Solidi A* **201**, 1302 (2004).
³T. Hasegawa and J. Takeya, *Sci. Technol. Adv. Mater.* **10**, 024314 (2009).
⁴H. Najafov, I. Biaggio, V. Podzorov, M. F. Calhoun, and M. E. Gershenson, *Phys. Rev. Lett.* **96**, 056604 (2006).
⁵H. Najafov, B. Lyu, I. Biaggio, and V. Podzorov, *Phys. Rev. B* **77**, 125202 (2008).
⁶O. Mitrofanov, D. V. Lang, C. Kloc, J. M. Wikberg, T. Siegrist, W.-Y. So, M. A. Sergent, and A. P. Ramirez, *Phys. Rev. Lett.* **97**, 166601 (2006).
⁷H. Najafov, B. Lee, Q. Zhou, L. C. Feldman, and V. Podzorov, *Nature Mater.* **9**, 938 (2010).
⁸R. G. Kepler, J. C. Caris, P. Avakian, and E. Abramson, *Phys. Rev. Lett.* **10**, 400 (1963).
⁹V. Ern, P. Avakian, and R. E. Merrifield, *Phys. Rev.* **148**, 862 (1966).
¹⁰F. V. M. Pope and N. E. Geacintov, *Mol. Cryst. Liq. Cryst.* **6**, 83 (1969).
¹¹R. K. T. Gentry, *J. Phys. Chem.* **81**, 3014 (1994).
¹²D. K. K. Liu and L. R. Faulkner, *J. Am. Chem. Soc.* **99**, 4594 (1977).
¹³O. Mitrofanov, C. Kloc, T. Siegrist, D. V. Lang, W.-Y. So, and A. P. Ramirez, *Appl. Phys. Lett.* **91**, 212106 (2007).
¹⁴C. Kloc, K. J. Tan, M. L. Toh, K. K. Zhang, and Y. P. Xu, *Appl. Phys. A* **95**, 219 (2009).
¹⁵J. L. Hall, D. A. Jennings, and R. M. McClintock, *Phys. Rev. Lett.* **11**, 364 (1963).
¹⁶M. Pope and C. Swenberg, *Electronic Processes in Organic Crystals and Polymers* (Oxford University Press, 1999).
¹⁷P. Irkhin and I. Biaggio, *Phys. Rev. Lett.* **107**, 017402 (2011).
¹⁸A. Saeki, S. Seki, T. Takenobu, Y. Iwasa, and S. Tagawa, *Adv. Mater.* **20**, 920 (2008).
¹⁹S. Tao, H. Matsuzaki, H. Uemura, H. Yada, T. Uemura, J. Takeya, T. Hasegawa, and H. Okamoto, *Phys. Rev. B* **83**, 075204 (2011).
²⁰K. Itoh and K. Honda, *Chem. Phys. Lett.* **87**, 213 (1982).
²¹A. Yildiz, P. T. Kissinger, and C. N. Reilly, *J. Chem. Phys.* **49**, 1403 (1968).
²²J. J. Burdett, A. M. Muller, D. Gosztola, and C. J. Bardeen, *J. Chem. Phys.* **133**, 144506 (2010).
²³V. V. Tarasov, G. E. Zorinians, A. I. Shushin, and M. M. Triebel, *Chem. Phys. Lett.* **267**, 58 (1997).
²⁴M. Cai, Y. Chen, J. Shinar, O. Mitrofanov, C. Kloc, and A. P. Ramirez, *Proc. SPIE* **7415**, 74151Y (2009).
²⁵P. M. Zimmerman, Z. Zhang, and C. B. Musgrave, *Nature Chem.* **2**, 648 (2010).
²⁶J. Kalinowski, *Organic Light Emitting Diodes: Principles, Characteristics, and Processes* (Marcel Dekker, New York, 1999).
²⁷A. M. Müller, Y. S. Avlasevich, W. W. Schoeller, K. Müllen, and C. J. Bardeen, *J. Am. Chem. Soc.* **129**, 14240 (2007).
²⁸H. Najafov, B. Lyu, I. Biaggio, and V. Podzorov, *Appl. Phys. Lett.* **96**, 183302 (2010).
²⁹B. A. Gregg, *J. Phys. Chem. B* **107**, 4688 (2003).
³⁰V. I. Arkhipov and H. Bässler, *Phys. Status Solidi A* **201**, 1152 (2004).
³¹A. Hangleiter, *Phys. Rev. B* **37**, 2594 (1988).
³²C.-H. Chen and H.-F. Meng, *Phys. Rev. B* **64**, 125202 (2001).